Progress In Electromagnetics Research C, Vol. 118, 83–97, 2022

High Gain Array Antenna Using Electromagnetic Band Gap Structures for 5G Applications

Sanae Dellaoui[1, *], Abdelmoumen Kaabal[2], Mustapha El Halaoui[1], Adel Asselman[1], Saida Ahyoud[2], and Loubna Rmili[1]

Abstract—This paper proposes a high gain array antenna operating in the Ku-band at 17.5 GHz for 5G applications. This new antenna is printed on an FR-4 substrate of thickness $h = 0.8$ mm and realized by changing the geometric shape of a rectangular patch, obtained by inserting an L-shaped slot to enlarge the bandwidth (1.5 GHz) and to increase the gain. To further enhance the gain, we used a 1×2 patch antenna array closely spaced and powered by a 1-to-2 Wilkinson power divider. We inserted two high-impedance surface (HIS) structures between the radiating elements and added two electromagnetic band gap (EBG) layers above the antenna. The antenna gain increases from 7.56 dB to 14.8 dB. The design and simulation have been performed by CST Microwave. A minor difference was noted between the measured and simulated data, where a slight shift was observed in the antenna's resonance frequency, which can be caused by fabrication tolerances or measurement error, uncertainty of the thickness of the FR4 substrate, and quality of SMA connector used. The final array antenna shows a directional radiation pattern with a gain of 14.8 dB and good radiation efficiency over the operating band.

1. INTRODUCTION

5G is the coming fifth-generation wireless technology based on the 802.11ac standard. It will allow us to respond to the explosion of our data consumption, so it will first of all avoid the saturation of the 4G network and also allow a significant increase in speed. To understand the interest of 5G, there are three important words to remember. The first is the rate, which will enable much faster Internet connection speeds than 4G and will be up to 10 times faster. The second latency is the reaction time between the moment you place an order and the moment it appears on the screen, and it will go from 10 to 1 ms. The third density: 5G will be able to support 1 million devices per square kilometer, a 10-fold increase in connection density. The 5G mobile network will enable a revolution in uses. In particular, it will promote the development of the Internet of Things. Then, thanks to its low latency, 5G will find a large number of applications, with upheavals in the field of health (telemedicine), transport (autonomous vehicles), the smart city (energy management), or the factories of the future (automation) [1–3].

The high gain antennas have been gaining much attention due to their properties to augment the rate of data transmitted per second. What is known about the gain is largely interesting for 5G applications. So one of the main techniques to enhance the gain is using an antenna array [4–6], but with the rapid development of multi-antenna systems, electromagnetic interference between antenna elements is one of the most concerned problems. Moreover, mutual coupling caused by surface waves has a serious effect on antenna array performances, such as radiation pattern, gain, and operating bandwidth [7–9]. It is essential to find suitable methods to reduce the mutual coupling and improve the performance of

Received 15 November 2021, Accepted 20 January 2022, Scheduled 2 February 2022
* Corresponding author: Sanae Dellaoui (sanae.dellaoui@gmail.com).
[1] Optics and Photonics Team, Faculty of Sciences, AbdelmalekEssaadi University, P. O. Box: 2121, Tetouan, Morocco. [2] Information Technology and Systems Modeling Team, FS, AbdelmalekEssaadi University, Tetouan, Morocco.

antenna array, to name only a few: optimizing the patch shape [10], adding the HIS (High Impedance Surface) between the antenna elements [11–14], and placing an additional electromagnetic band gap (EBG) dielectric layer over the patch [13, 15, 16].

In recent years, there has been considerable interest in high-impedance surfaces for enhancement of antennas [17–20]. HIS structures are periodic and widely used, especially for antenna applications [21–23], and they may be realized by etching or drilling on the metal or dielectric substrates to improve the performance of antennas, especially the gain/radiation patterns by putting an end to the problems created by surface waves [11, 24–26].

An EBG was chosen because it is also one of the most practical ways to increase the gain of the antenna [15, 27, 28]. EBG dielectrics are generally located half wavelength above ground plane with a quarter dielectric wavelength thicknesses. The coupling between the antenna and EBG produces a most directive radiation pattern. Unfortunately, low radiation bandwidth is the major disadvantage of the antenna using EBG layers.

In this paper, a new patch array antenna is configured. We started by a rectangular patch antenna, and we changed its shape by inserting an L-shaped slot to have a wide bandwidth and increase the gain from 5.79 dB to 7.5 dB. To increase the gain further, we used the two elements of the array antenna and added two HIS Structures in the middle of array to suppress the surface waves created between the radiated elements. For that the gain is enhanced at 9.88 dB, and to augment the gain more and to have a directional radiation by adding two EBG layers of thickness $\approx \lambda_g/4$ above the array antenna a distance around $\lambda/2$ and a distance between the couches is near $\lambda/4$ [15, 16, 21, 29]. The gain improves up to 14.8 dB, and we notice that the bandwidth has become narrower when we add the EBG layers, that's why it was necessary to have a wide bandwidth starting patch.

The performance comparison analysis of the proposed antenna with other Ku band antennas is summarized in Table 1; the proposed design is highly attractive due to its much better performance in terms of gain and impedance bandwidth.

Table 1. Comparison of proposed antenna performance with other compact antennas.

Ref.	Size (mm^2)	Substrate	Relative Permittivity	Resonance Frequency (GHz)	Bandwidth (GHz)	Gain (dB)
[30]	9.39×7.1	Taconic TLT-8	2.55	14.24	0.5	5.7
[31]	10×10	Rogers RO4350	3.66	13.5	0.37	5.14
[32]	14.8×11.6	Taconic TLY-5	2.2	16.2	1.123	6.1
[33]	17×17	FR-4	4.9	15.8	1.23	4.45
[34]	20×20	Duriod 5870	2.33	15.46	1.07	1.97
Proposed Antenna	20×20	FR-4	4.3	17.5	1.34	7.56

2. ANTENNA CONFIGURATION

2.1. Antenna Development

We started with a classic rectangular patch antenna (Fig. 1(a)) fed by a microstrip line 50 Ω of length $L_f = 10$ mm and $W_f = 1.5$ mm, printed on an FR-4 substrate (relative permittivity $\varepsilon = 4.4$, loss tangent $\tan\delta = 0.025$, and thickness $h = 0.8$ mm) $W = 20$ mm, $L = 20$ mm, $h = 0.035$ mm. The ground plane is

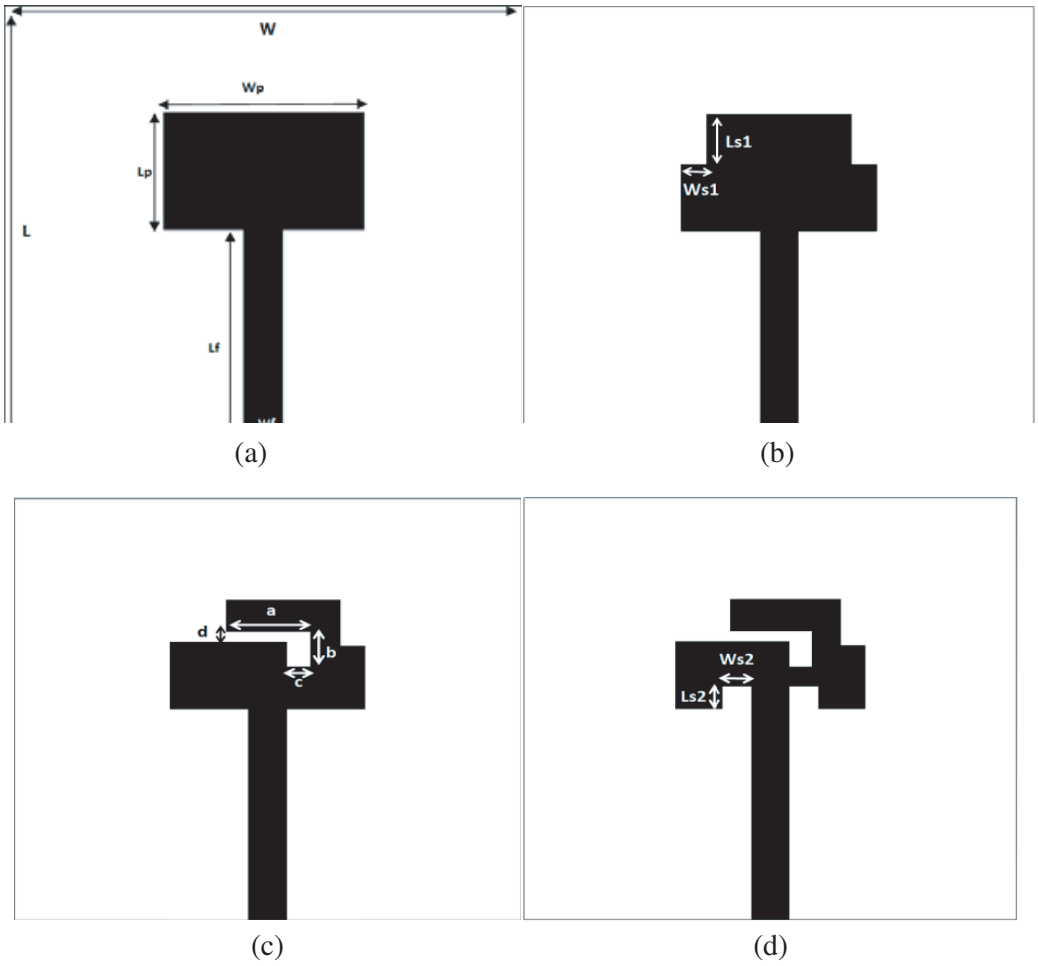

Figure 1. Evolution design of the proposed rectangular patch antenna. (a) Rectangular patch antenna. (b) Antenna #1. (c) Antenna #2. (d) Proposed antenna.

a total mass of the same substrate size. Two rectangular notches have been added on the upper corners of the patch with $W_{s1} = 1\,\text{mm}$, $L_{s1} = 2.2\,\text{mm}$ (Fig. 1(b)) and another L-shaped slit inserted in the radiating patch, with dimensions: $a = 3.3\,\text{mm}$, $b = 1.2\,\text{mm}$, and $c = 0.95\,\text{mm}$, as shown in (Fig. 1(c)), and by cutting two slots at the input level of the radiating patch with $W_{s2} = 1.2\,\text{mm}$ and $L_{s2} = 1.1\,\text{mm}$ (Fig. 1(d)), the proposed antenna characteristics are much improved, such as impedance bandwidth and gain.

The antenna was designed and simulated by CST software. All optimum dimensions are shown in the following Table 2.

Table 2. The optimal values of the patch antenna parameters.

Parameter	Value	Parameter	Value
h_s	0.8	$L = W$	20
W_p	7.7	L_p	5.2
L_{s1}	2.2	W_{s1}	1
a	3.2	B	1.2
c	0.95	D	0.5
W_{s2}	1.2	L_{s2}	1.1

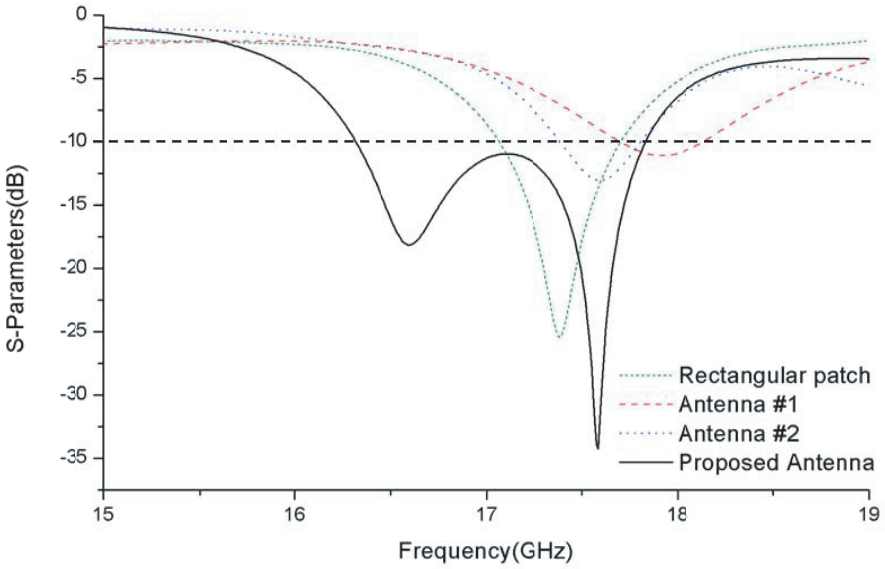

Figure 2. Simulated S_{11} for prototypes Rectangular Antenna, Antenna #1, Antenna #2 and Proposed Antenna.

Fig. 2 shows the reflection coefficient as a function of frequency of each antenna. There is the minimum reflection at -10 dB, and Table 3 shows the comparison of the evolution process of the proposed patch antenna.

Table 3. Comparison of the evaluation process of the proposed patch antenna.

	Resonance Frequency (GHz)	**Bandwidth (GHz)**	**Gain (dB)**
Rectangular patch antenna	17.5	0.6	5.79
Antenna#1	18	0.44	5.67
Antenna#2	17.6	0.42	7.03
Proposed antenna	17.5	1.34	7.56

The rectangular antenna is adapted to the frequency of 17.5 GHz with bandwidth 600 MHz. To enhance the bandwidth and the gain, we added two rectangular notches to the start antenna on the upper corners, but we find that the resonance moves to 18 GHz, and the bandwidth and gain decrease a bit (0.44 GHz). For that we inserted an L-shaped slit in the radiating patch, and the antenna is adapted to 17.6 GHz and the gain enhanced to 7 dB. We need a large bandwidth for the next step. So to improve it, we cut two slots at the input level of the patch. The proposed antenna gave more optimal results; it is well adapted to the 17.5 GHz frequency with a bandwidth of 1.34 GHz and the gain of 7.56 dB.

2.2. *b*-Parametric Study

2.2.1. Variation Effect in Slot Width W_{S1} and Length L_{s1}

Fig. 3 shows the effect of the variation of parameter W_{s1} on return loss characteristics. We find that the antenna adaptation and impedance bandwidth at 17.5 GHz are optimal at the value of $W_{s1} = 1$ mm. The figure also shows that, in the frequency band between 16.32 GHz and 17.83 GHz, the return amplitude is -34 dB. According to Fig. 4, we notice that the length L_{s1} does not influence the characteristics of the parameter S_{11} and the bandwidth. For this reason, the value $L_{s1} = 2.2$ mm has been chosen.

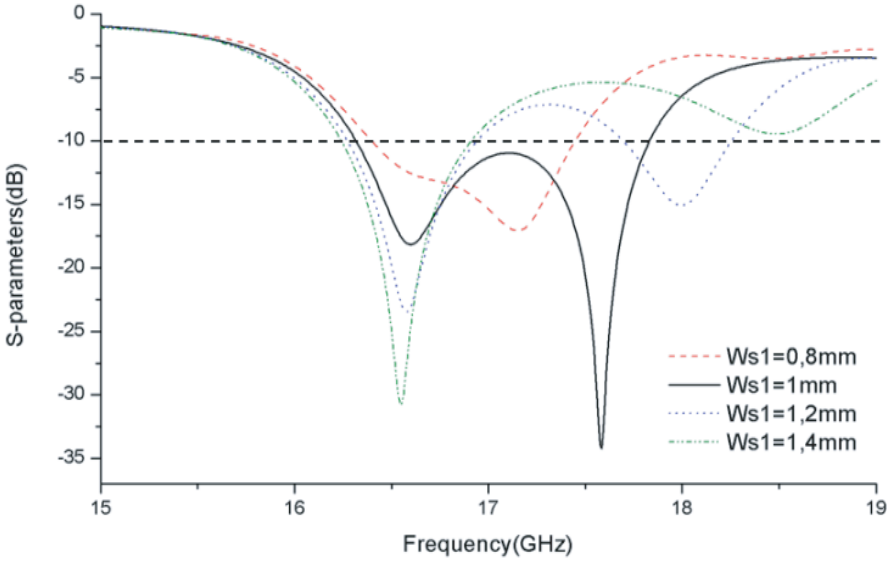

Figure 3. Effect of varying the width 'W_{s1}' on return loss.

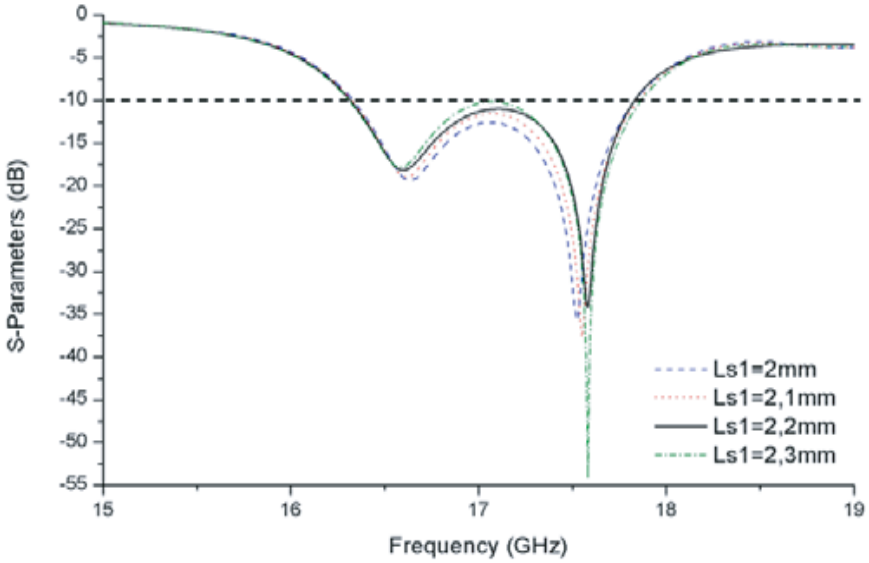

Figure 4. Effect of varying the length 'L_{s1}' on return loss.

2.2.2. Effect of Varying the Size of the L-Shaped Slot

The effects of the variation in the total length of the L-shaped slot, i.e., dimensions 'a', 'b', and 'c', on the return loss are depicted in the following figures (Fig. 5, Fig. 6 and Fig. 7). The figures show that the optimal values of 'a', 'b', and 'c' are successively 3.2 mm, 1.2 mm, and 0.95 mm. These values give the resonant frequency at 17.5 GHz, maximum return loss amplitude, and a wider band of 1.5 dB. As the width increases the adaptation of the antenna and the impedance bandwidth at 17.5 GHz improve.

2.3. Array Antenna

Figure 8 shows the geometry and photograph of the 2-element antenna array fed by a 1-to-2 Wilkinson power divider. The array has an overall size of $L_a \times W_a = 40 * 40$ mm. The spacing between antenna

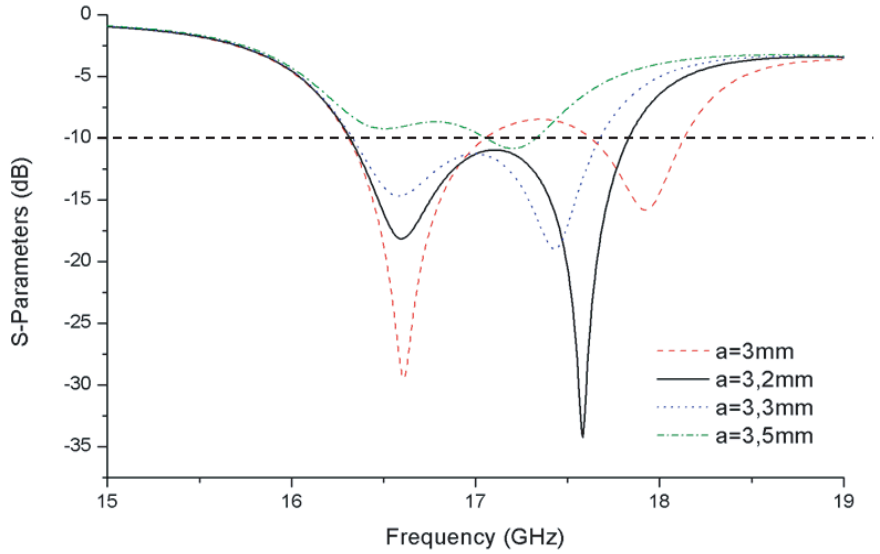

Figure 5. Effect of varying the length 'a' on return loss.

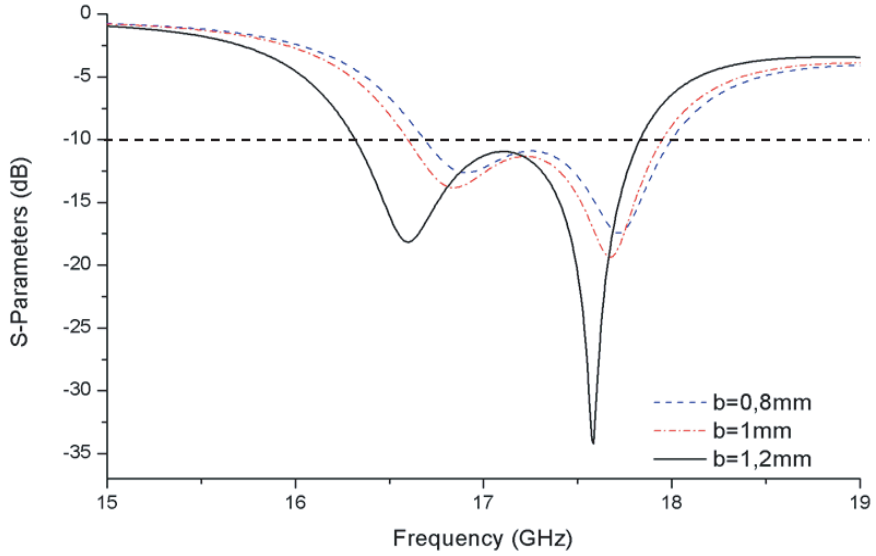

Figure 6. Effect of varying the length 'b' on return loss.

elements is set to $S = 7.8\,\text{mm}$, which is almost a half of a free space wavelength $\lambda/2$ at 17.5 GHz. The array has been designed, optimized, and simulated using CST Microwave Studio.

The simulated and measured results of the reflection coefficients S_{11} for the proposed two-element antenna array are illustrated in Fig. 9. It is apparent that the proposed array antenna has a good impedance matching at the desired frequency band of 17.5 GHz for S_{11} less than $-10\,\text{dB}$ with the operating bandwidth 1.33 GHz. The measured resonant frequencies of proposed array shift slightly compared with the simulated resonant frequencies from 17 GHz (fabricated prototype) to 17.5 GHz (simulated case), which can be caused by fabrication precision and the excess of soldering material on the Wilkinson feed. Fig. 10 illustrates simulated radiation pattern, (a) elevation plane pattern, (b) azimuth plane pattern of the array antenna; we show that the gain increases more until 8.91 dB.

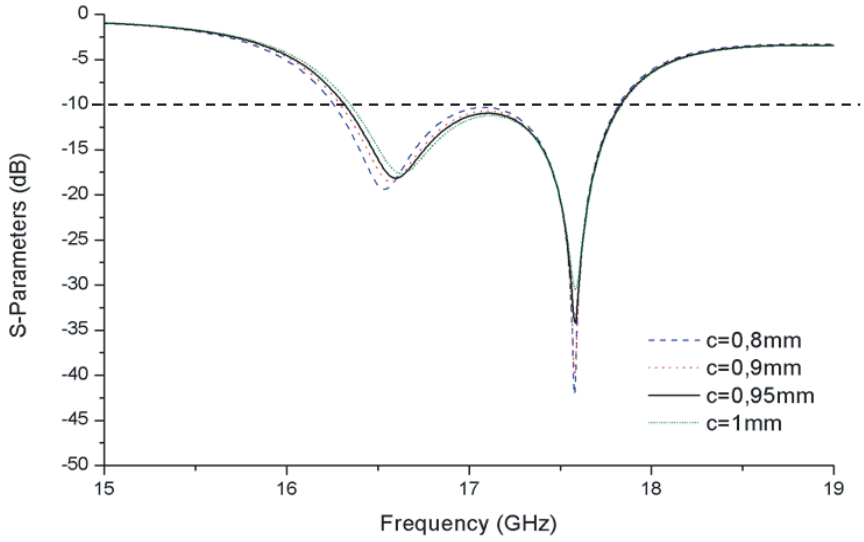

Figure 7. Effect of varying the length 'c' on return loss.

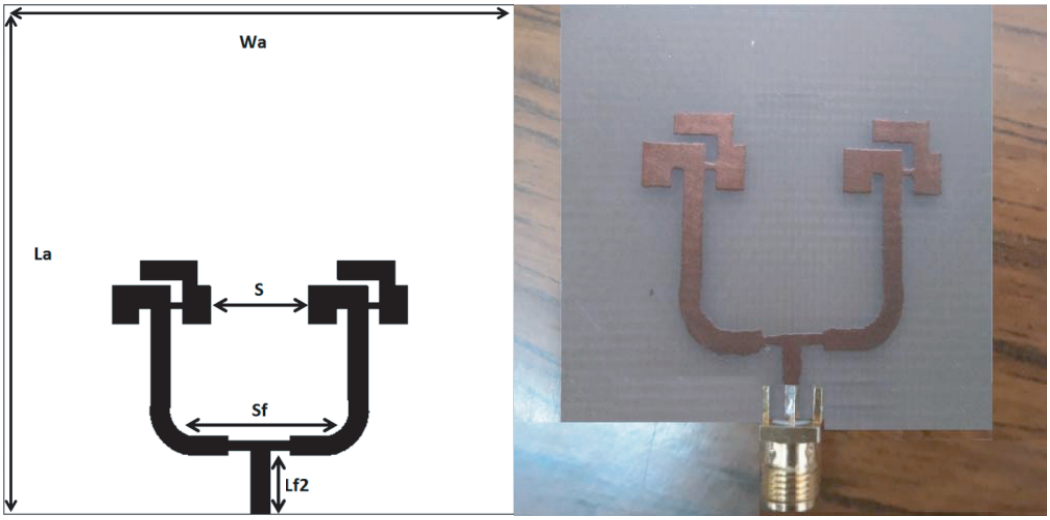

(a) (b)

Figure 8. Geometry of the proposed patch array antenna design. (a) Array layers. (b) Photograph of fabricated prototype.

3. INCREASING THE ANTENNA GAIN

3.1. Addition of HIS

High-Impedance Surface (HIS) consists of four parts: a ground plane, a dielectric substrate, metal patch, and connection via. HIS structures are used to cancel the mutual coupling between the antennas and then improve the gain. Fig. 11 shows a unit cell of the HIS structure. The parameters of the HIS structure are optimized and marked on the figure, and their values are given in Table 4. The reflection phase (Fig. 12) of the HIS structure shows a stopband obtained in the frequency range 10 GHz to 18 GHz with a reflection phase in the range of $+90° \pm 45°$.

To improve the performance of antenna by deleting the surface waves between elements of array,

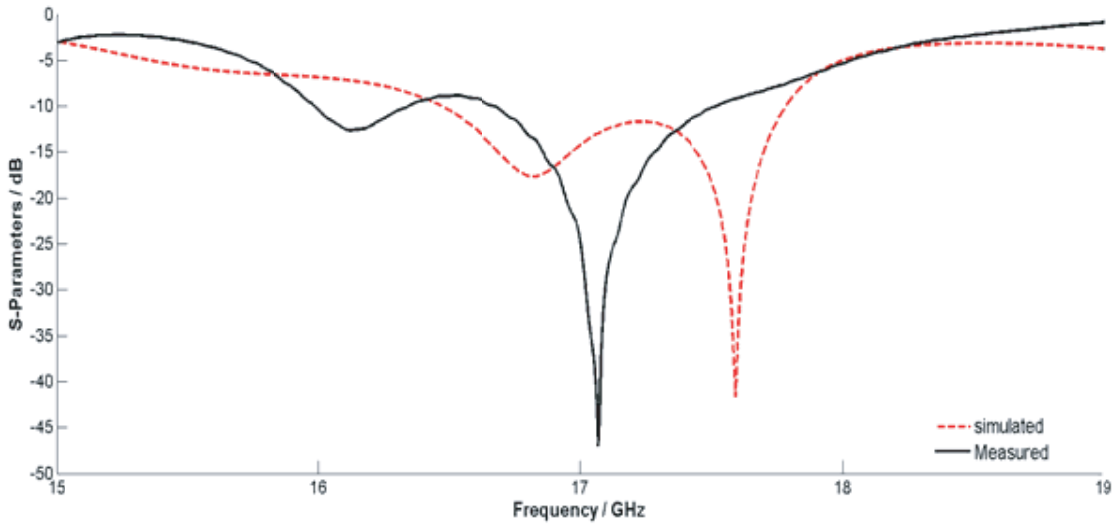

Figure 9. Simulated and measured return loss of the proposed antenna.

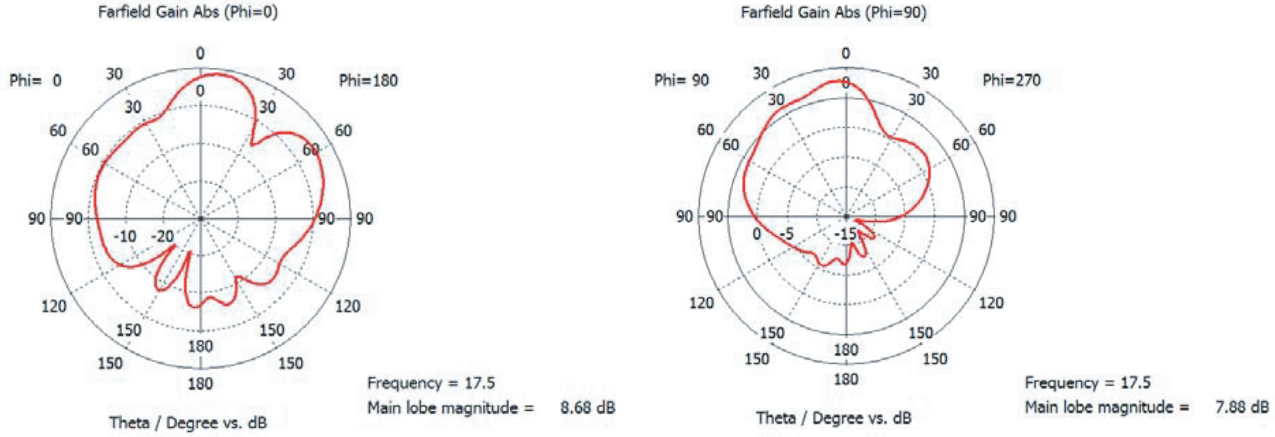

(a) (b)

Figure 10. Radiation pattern, (a) elevation plane pattern, (b) azimuth plane pattern.

Table 4. Optimal values of the HIS parameters.

Parameters	Value (mm)	Parameters	Value (mm)
W_h	5.1	H_h	0.5
L_h	5.1	G_h	0.8
W_{h1}	2.75	H_{h1}	0.3
L_{h1}	0.75		

Fig. 13 depicts the integration of the HIS structure in the antenna array. The three cases of the proposed antenna with HIS are: the first case using two HISs between two patches, the second one, by adding four HISs, and the third, to merge the two previous cases.

The following Fig. 14 shows the effect of variation in the number of HISs on the antenna array. As the number of HIS structures around antenna array increases, the resonance moves away from the 17.5 GHz frequency. So the best structure is with two HISs which is well adapted and improves the

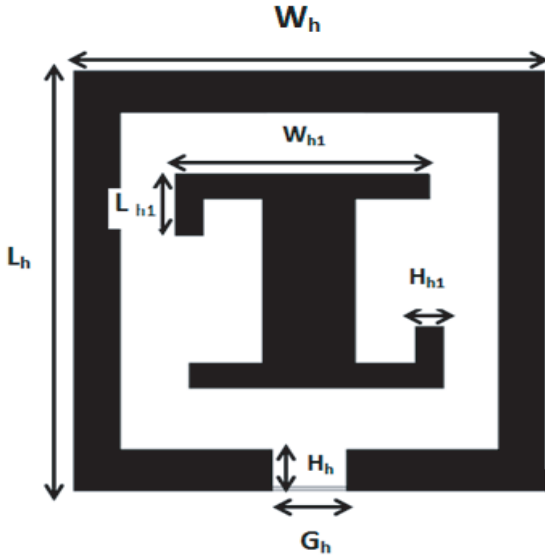

Figure 11. Unit cell of the HIS structure.

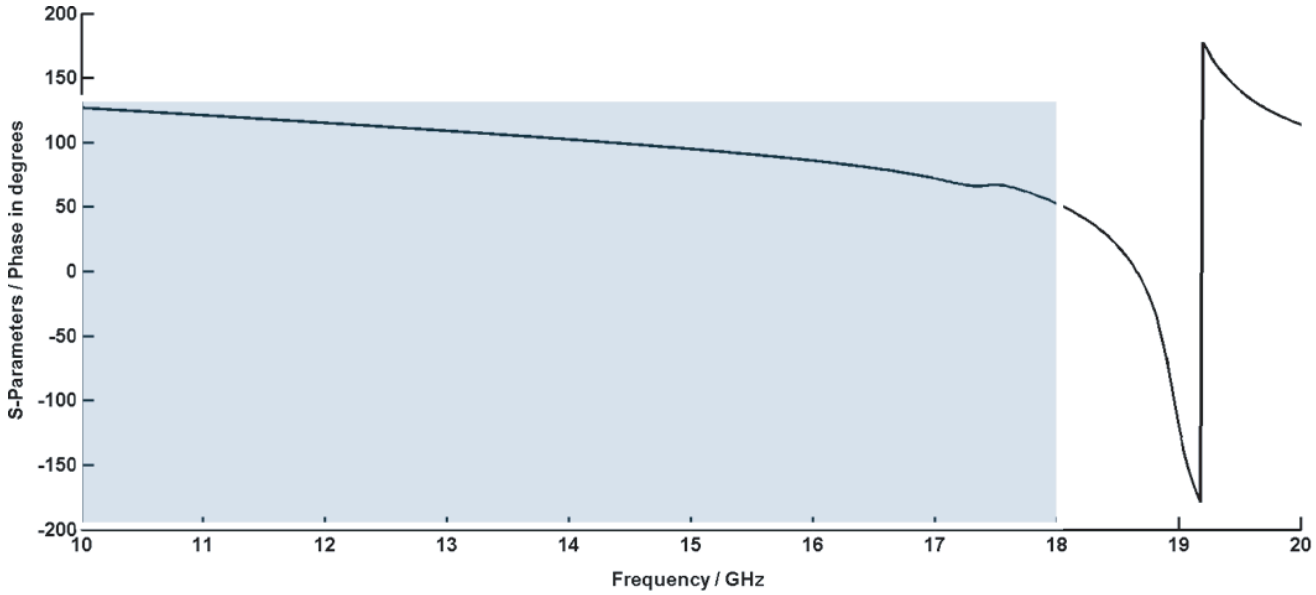

Figure 12. The reflection coefficient phase.

characteristics of the array. Fig. 15 depicts the radiation pattern of the array antenna with two HISs, the gain increases from 8.90 dB up to 9.88 dB.

3.2. Addition of EBG Layers

Two EBG (Electromagnetic Band Gap) dielectric layers FR-4 of a thickness $d \approx \lambda_g/4$ were added to our array over the radiating elements at a distance $H \approx \lambda/2$ (see Fig. 16). Multiple reflections that happen between the patches and EBG superstrate provide a spatial filtering for focusing the main beam radiation of the antenna that allows enhancement for the antenna gain. By observing the return loss coefficient of the antenna array with and without HIS structure and EBG superstrate (Fig. 17), it can be seen that as the number of EBG layers increases the bandwidth decreases, but the antenna remains adapted to the 17.5 GHz frequency. The radiation patterns of the proposed array antenna at 17.5 GHz

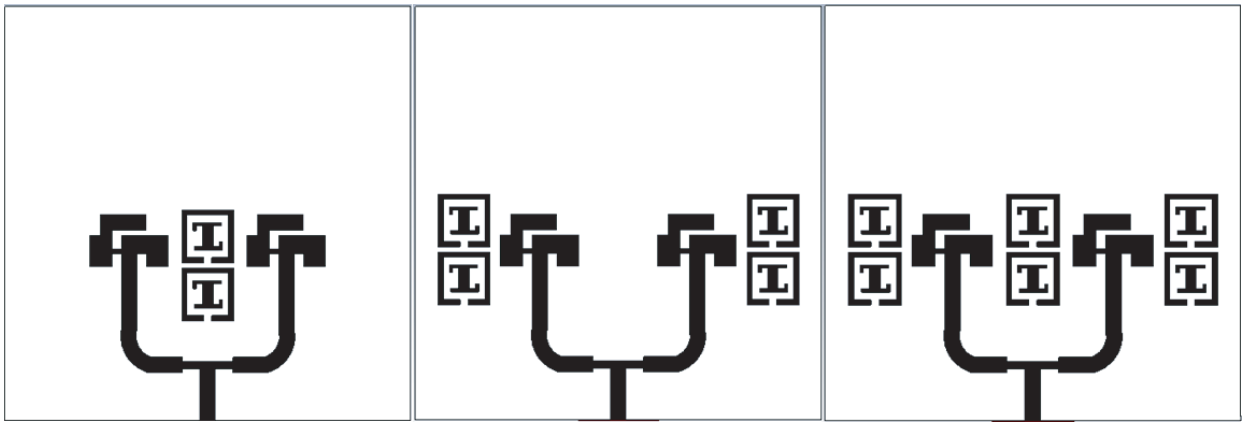

Figure 13. Different cases for the variation in the number of HIS unit cells.

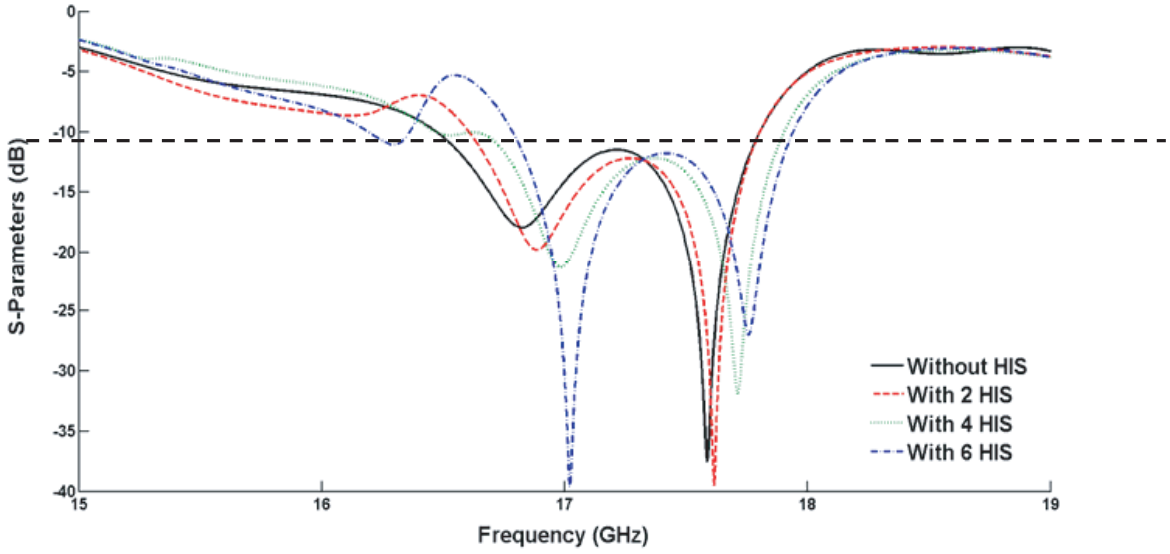

Figure 14. Simulated S_{11} of the array with and without HIS.

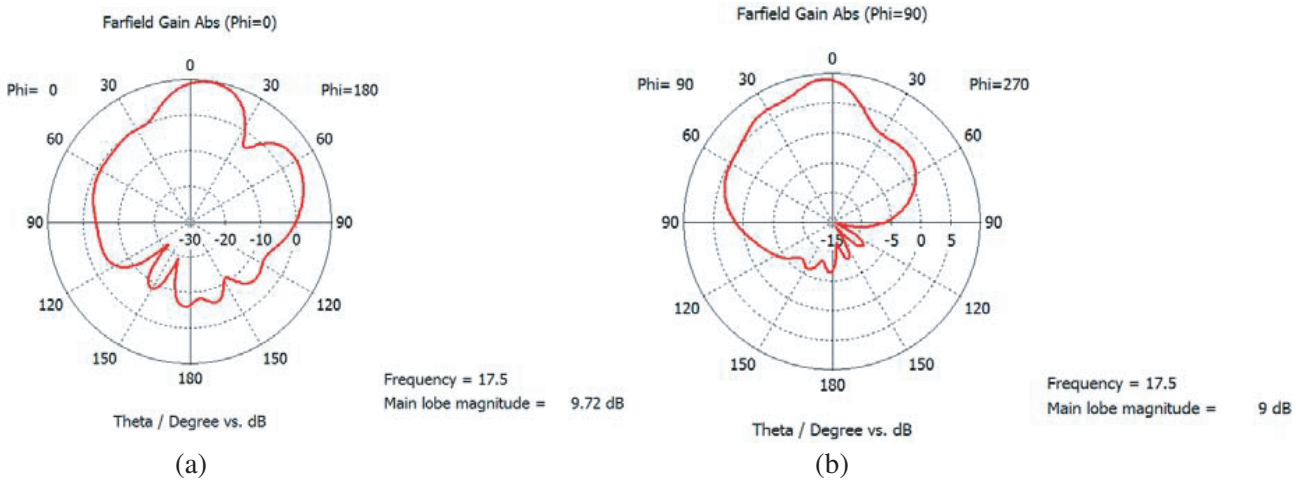

(a) (b)

Figure 15. Radiation pattern, (a) elevation plane pattern, (b) azimuth plane pattern.

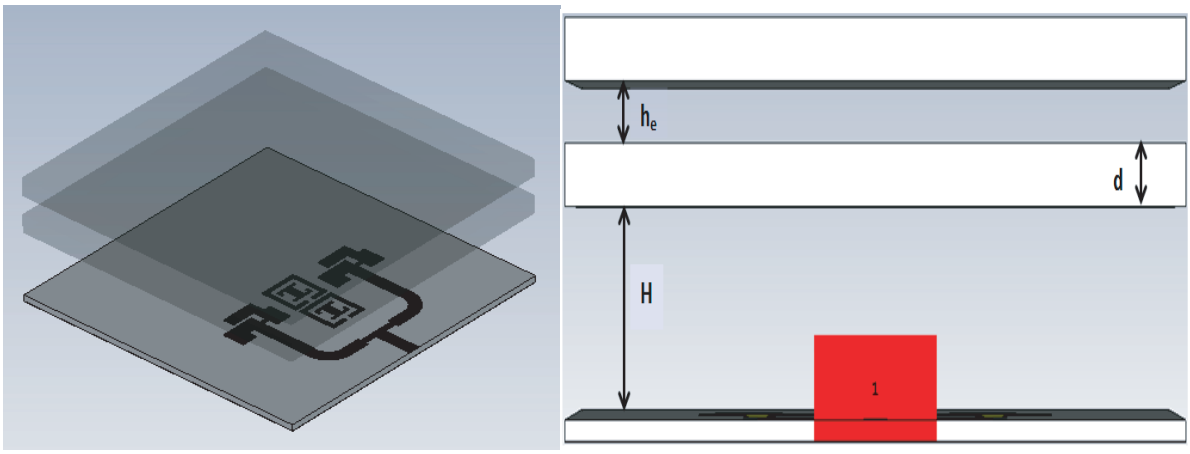

Figure 16. Array antenna with two EBG superstrate dielectric.

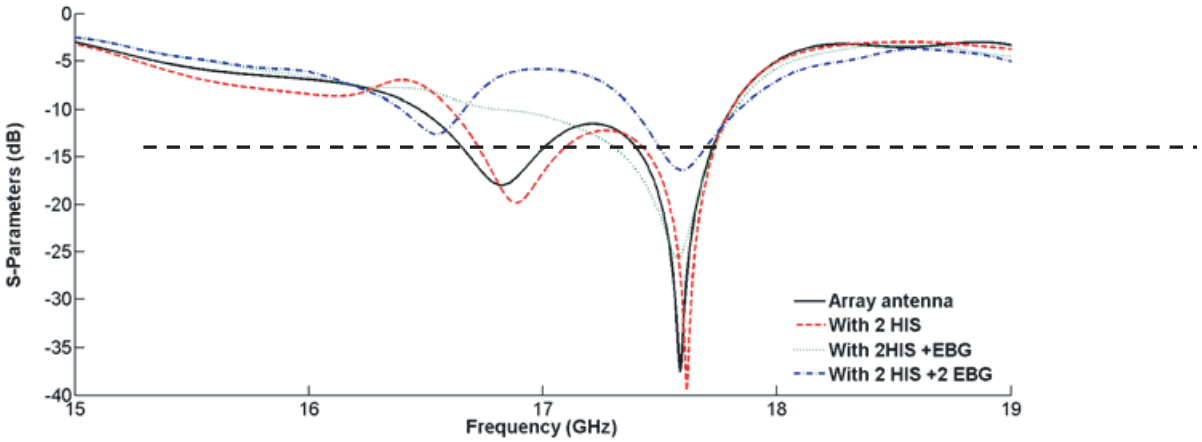

Figure 17. Simulated S_{11} of the array with and without EBG.

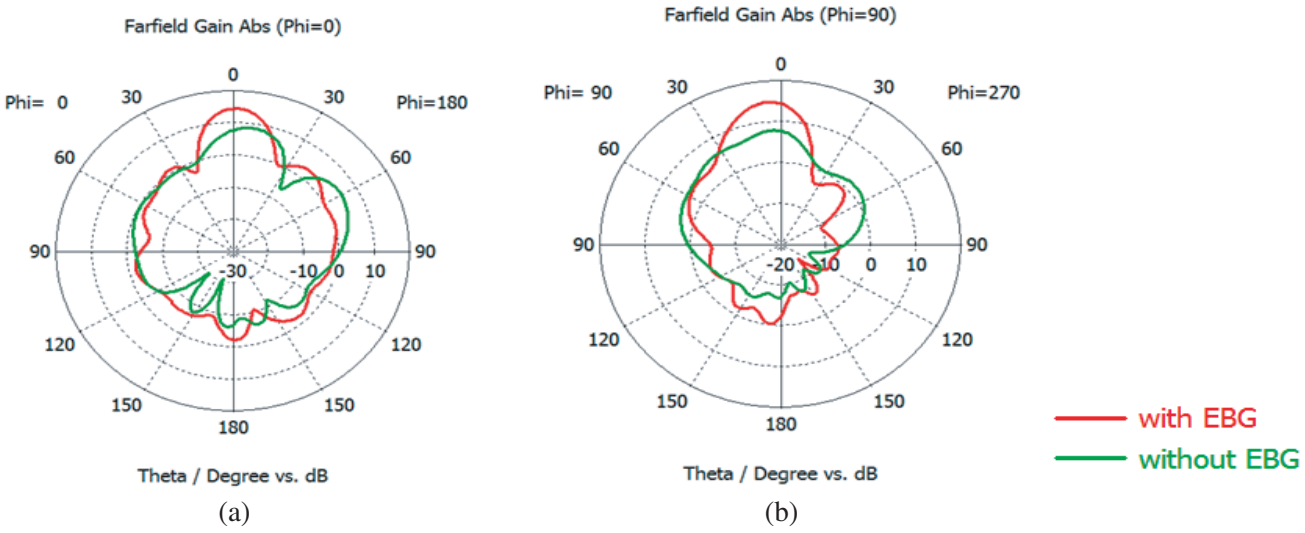

(a) (b)

Figure 18. Radiation pattern, (a) elevation plane pattern, (b) azimuth plane pattern.

are depicted in Fig. 18. The gain increases from 8.9 dB until 14.8 dB, and the increase depends on the number of EBG layers. The radiation patterns of the proposed array antenna at 17.5 GHz for the elevation plane pattern and azimuth plane pattern are illustrated in Fig. 18. It can be seen that the antenna almost achieves directional radiation pattern over the 17.5 GHz when the EBG superstrate is used. Fig. 19 gives the radiation efficiency of the final antenna versus frequency. An improvement is observed in the efficiency of antenna when the EBG layers are added in which the radiation efficiency reaches values around 80% [35].

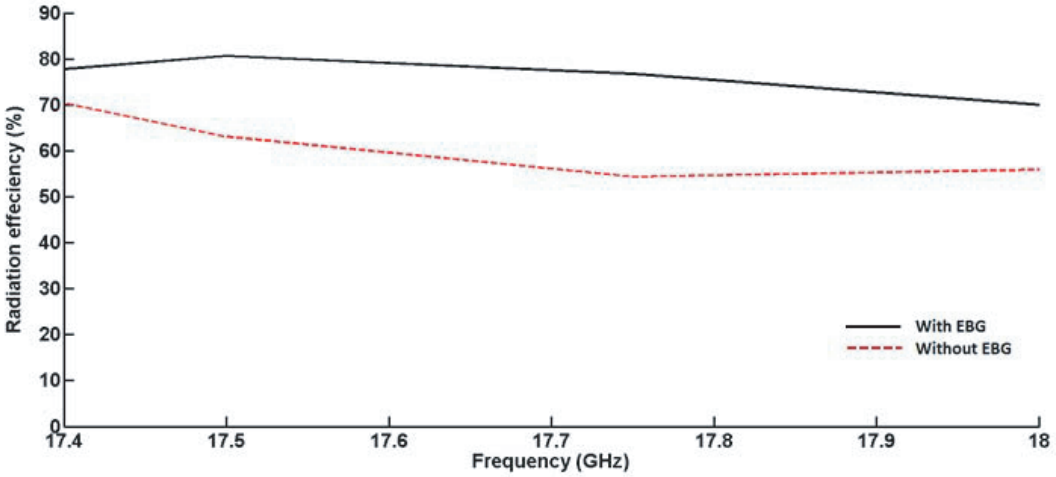

Figure 19. Radiation efficiency with and without EBG.

Table 5 shows the performance comparison among designed patch antennas. We can see that the gain increases in every stage except the band which became narrower when we added the two EBG layers.

Table 5. Performance comparison among designed patch antennas.

Performance Parameters	1 patch antenna	Array antenna	Array antenna +2HIS	Array antenna +2HIS+2EBG
Reflection coefficient (dB)	−33.5	−37.39	−35.85	−16.36
Bandwidth (GHz)	1.34	1.33	1.25	0.45
Gain (dB)	7.56	8.9	9.88	14.80
Radiation efficiency(%)	81.5	81	84	82.5

Fig. 20 shows the surface current distribution of the array antenna at frequency 17.5 GHz, and the maximum current density is indicated by the red color while the minimum current density is indicated by blue color. The currents mainly distribute along the edges of the array antenna (Fig. 20(a)). In the antenna array with EBG and HIS we see that the currents are distributed in all the antenna, which means that the HIS cancels the mutual couplings.

Figure 21 shows the simulated RCS of rectangular antenna, proposed patch, and proposed array antenna. We see that RCS has increased from −7 dBm to 15 dBm at the frequency 17.5 GHz, which is one of the inconveniences of our antenna network. So it is necessary to find a technique to decrease RCS in the next work.

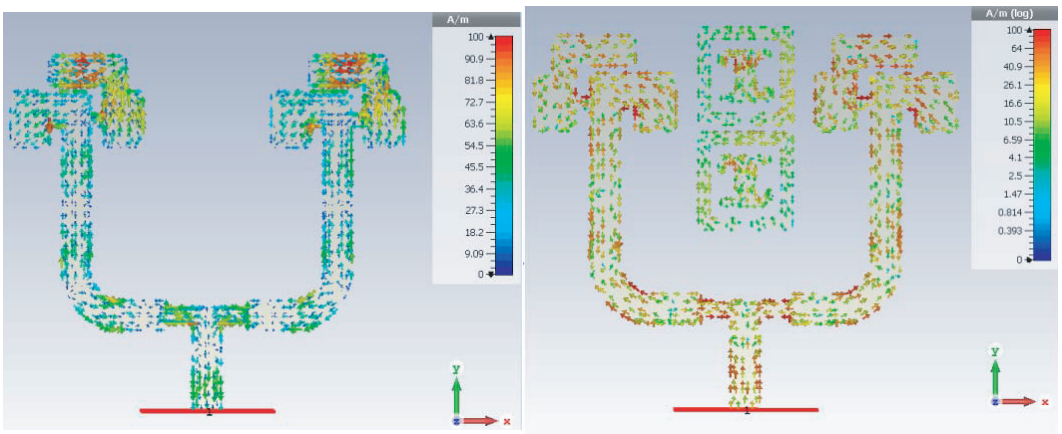

(a) (b)

Figure 20. Surface current distribution of the array antenna: (a) without EBG and HIS, (b) with EBG and H.

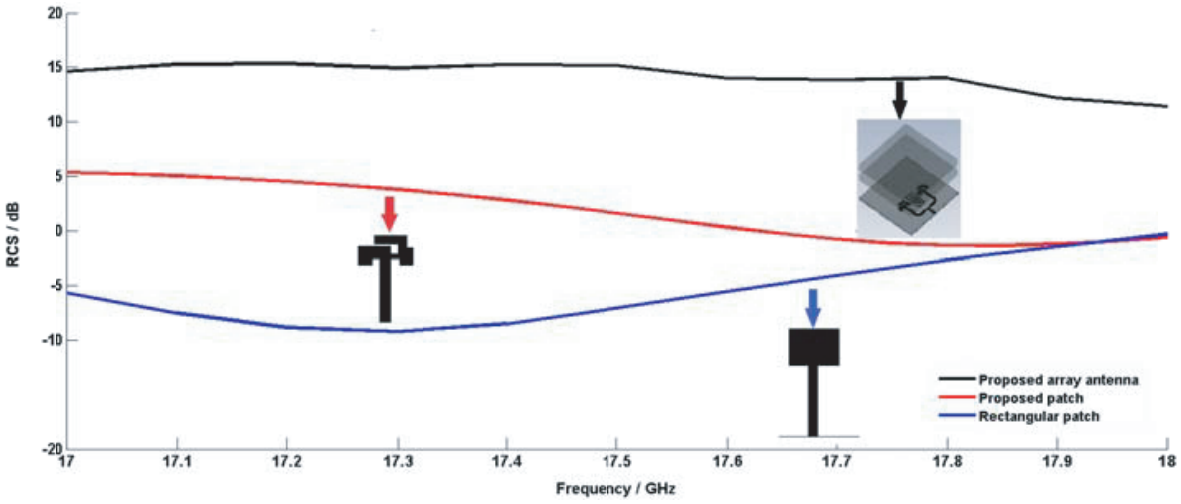

Figure 21. Comparison of Simulated RCS versus frequency of rectangular antenna, proposed patch and proposed array antenna.

4. CONCLUSION

In this paper, we have designed a new Ku-band microstrip patch antenna. To increase the bandwidth (1.5 GHz) and gain, an L-shaped slot was added to the patch. To have a higher gain we used an array of 2-elements and adding HIS structures and EBG layers. The final antenna has a greater gain than 14.8 dB. Our work clearly has some limitations in the radiation bandwidth by using the EBG; it becomes narrower, which is why it was necessary to configure the start patch antenna with a wider bandwidth for the final bandwidth to be acceptable. For that it is possible to operate the antenna for the Ku-band application.

ACKNOWLEDGMENT

We gratefully acknowledge Dr. Naima A. Touhami from Electronics Instrumentation and microwave Laboratory, Faculty of Sciences Tetouan, AbdelmalekEssaadi University, for the measurement and the technical assistance in our experimental work.

REFERENCES

1. Andrews, J. G., et al., "What will 5G be?" *IEEE Journal on Selected Areas in Communications*, Vol. 32, No. 6, 1065–1082, Jun. 2014.
2. Hajlaoui, E., A. Zaier, A. Khlifi, J. Ghodhbane, M. B. Hamed, and L. Sbita, "4G and 5G technologies: A comparative study," *2020 5th International Conference on Advanced Technologies for Signal and Image Processing (ATSIP)*, 16, Sousse, Tunisia, Sept. 2020.
3. Song, et al., "Research on 4G and 5G authentication signaling.pdf," 2019.
4. Haraz, O. M., A. Elboushi, S. A. Alshebeili, and A.-R. Sebak, "Dense dielectric patch array antenna with improved radiation characteristics using EBG ground structure and dielectric superstrate for future 5G cellular networks," *IEEE Access*, Vol. 2, 909–913, 2014.
5. Al-Tarifi, M. A., D. E. Anagnostou, A. K. Amert, and K. W. Whites, "Bandwidth enhancement of the resonant cavity antenna by using two dielectric superstrates," *IEEE Transactions on Antennas and Propagation*, Vol. 61, No. 4, 1898–1908, Apr. 2013.
6. Kishk, A. A., "DRA-array with 75% reduction in elements number," *2013 IEEE Radio and Wireless Symposium*, 70–72, Austin, TX, USA, Jan. 2013.
7. Abdulhameed, M. K., et al., "Novel design of triple bands EBG," *TELKOMNIKA (Telecommunication Computing Electronics and Control)*, Vol. 17, No. 4, 1683, Aug. 2019.
8. Khadom Mohsen, M., M. S. M. Isa, Z. Zakaria, A. A. M. Isa, M. K. Abdulhameed, and M. L. Attiah, "Control radiation pattern for half width microstrip leaky wave antenna by using PIN diodes," *International Journal of Electrical and Computer Engineering (IJECE)*, Vol. 8, No. 5, 2959, Oct. 2018.
9. Wong, S. W. and L. Zhu, "EBG-embedded multiple-mode resonator for UWB bandpass filter with improved upper-stopband performance," *IEEE Microwave and Wireless Components Letters*, Vol. 17, No. 6, 421–423, Jun. 2007.
10. Jackson, D. R., J. T. Williams, A. K. Bhattacharyya, R. L. Smith, S. J. Buchheit, and S. A. Long, "Microstrip patch designs that do not excite surface waves," *IEEE Transactions on Antennas and Propagation*, Vol. 41, No. 8, 1026–1037, Aug. 1993.
11. Kaabal, A., M. E. halaoui, S. Ahyoud, and A. Asselman, "A low mutual coupling design for array microstrip antennas integrated with electromagnetic band-gap structures," *Procedia Technology*, Vol. 22, 549–555, 2016.
12. Tony, et al., "Artificial dielectric superstrate loaded antenna F.pdf," 2019.
13. Huang and Fan, "Broadband and high-aperture efficiency Fabry-Perot A.pdf," 2021.
14. Dhull, D., "Design of triple band-notched UWB mimodiversity A.pdf," 2021.
15. Kaabal, A., et al., "Array antenna design with dual resonators 1D-EBG for enhancement of directivity and radiation bandwidth," 10, 2019.
16. Dellaoui, S., A. Kaabal, M. E. Halaoui, and A. Asselman, "Patch array antenna with high gain using EBG superstrate for future 5G cellular networks," *Procedia Manufacturing*, Vol. 22, 463–467, 2018.
17. Zhu, S. and R. Langley, "Dual-band wearable textile antenna on an EBG substrate," *IEEE Transactions on Antennas and Propagation*, Vol. 57, No. 4, 926–935, Apr. 2009.
18. Salonenet, P. and Y. Rahimat-Samii, "Effects of antenna bending on input matching and impedance bandwidth," 5, 2007.
19. Salonen, P., M. Keskilammi, and Y. Rahmat-Samii, "Textile antennas: Effect of antenna bending on radiation pattern and efficiency," *2008 IEEE Antennas and Propagation Society International Symposium*, 14, San Diego, CA, Jul. 2008.
20. Ferreira, D., P. Pires, R. Rodrigues, and R. F. S. Caldeirinha, "Wearable textile antennas: Examining the effect of bending on their performance," *IEEE Antennas Propag. Mag.*, Vol. 59, No. 3, 54–59, Jun. 2017.

21. Dellaoui, S., A. Asselman, S. Ahyoud, A. Kaabal, L. Rmili, and M. Elhalaoui, "Design of a new patch antenna using EBG structures and superstarte operating in the Ku-band for 5G cellular networks," *Mobile, Secure, and Programmable Networking*, Vol. 11557, 61–68, Renault, S. Boumerdassi, C. Leghris, and S. Bouzefrane, Éd., Springer International Publishing, Cham, 2019.
22. Karthikeya, G. S., M. P. Abegaonkar, and S. K. Koul, "Low cost high gain triple band mmWaveSierpinski antenna loaded with uniplanar EBG for 5G applications," *2017 IEEE International Conference on Antenna Innovations & Modern Technologies for Ground, Aircraft and Satellite Applications (iAIM)*, 15, Bangalore, India, Nov. 2017.
23. Arora, C., S. S. Pattnaik, and R. N. Baral, "Performance enhancement of patch antenna array for 5.8 GHz Wi-MAX applications using metamaterial inspired technique," *AEU — International Journal of Electronics and Communications*, Vol. 79, 124–131, Sept. 2017.
24. Farahani, H. S., M. Veysi, M. Kamyab, and A. Tadjalli, "Mutual coupling reduction in patch antenna arrays using a UC-EBG superstrate," *Antennas Wirel. Propag. Lett.*, Vol. 9, 57–59, 2010.
25. Leger, L., T. Monediere, and B. Jecko, "Enhancement of gain and radiation bandwidth for a planar 1-D EBG antenna," *IEEE Microwave and Wireless Components Letters*, Vol. 15, No. 9, 573–575, Sept. 2005.
26. Dalal, P. and S. K. Dhull, "Upper WLAN band notched UWB monopole antenna using compact two via slot electromagnetic band gap structure," *Progress In Electromagnetics Research C*, Vol. 100, 161–171, 2020.
27. Thevenot, M., M. S. Denis, A. Reineix, and B. Jecko, "Design of a new photonic cover to increase antenna directivity," *Microwave and Optical Technology Letters*, Vol. 7, No. 2, 136–139, 1999.
28. Mallahzadeh, A., A. Birhadi, and H. Bahrami, "Electromagnetic Band Gap (EBG) superstrate resonator antenna design for monopulse radiation pattern," *Applied Computational Electromagnetics Society Journal*, Vol. 27, No. 11, 908–917, 2012.
29. Qiuet, M. and S. He, "High-directivity patch antenna with both photonic bandgap substrate and photonic bandgap cover," *Microwave and Optical Technology Letters*, Vol. 30, No. 1, 41–44, Jul. 2001.
30. Parikh, H., S. V. Pandey, and M. Sahoo, "Design of a modified E-shaped dual band patch antenna for Ku band application," *2012 International Conference on Communication Systems and Network Technologies*, 49–52, Rajkot, Gujarat, India, May 2012.
31. Bhadouria, A. S., S. Kumari, and M. Kumar, "X-band and Ku-band patch antenna for radio location applications," *Proceedings of the International Conference on Recent Cognizance in Wireless Communication & Image Processing*, 897–904, N. Afzalpulkar, V. Srivastava, G. Singh, and D. Bhatnagar, Éd., Springer India, New Delhi, 2016.
32. Hasan, Md. I., S. A. H. Chowdhury, A. Khaleque, and M. A. Motin, "Experimental analysis of simple and low cost three band (C-band, Ku-band and K-band) compact patch antenna," *2013 International Conference on Informatics, Electronics and Vision (ICIEV)*, 14, Dhaka, Bangladesh, May 2013.
33. Bhadouria, A. S., S. Mieee, and M. Kumar, "Wide Ku-band microstrip patch antenna using defected patch and ground," 5, 2014.
34. Islam, M. M., M. T. Islam, and M. R. I. Faruque, "Dual-band operation of a microstrip patch antenna on a Duroid 5870 substrate for Ku- and K-bands," *The Scientific World Journal*, Vol. 2013, 110, 2013.
35. Abdulhameed, M. K., M. S. M. Isa, I. M. Ibrahim, M. K. Mohsin, S. R. Hashim, and M. L. Attiah, "Improvement of microstrip antenna performance on thick and high permittivity substrate with electromagnetic band gap," *Control Systems*, Vol. 10, 10, 2018.